

**Signatures of hadron-quark mixed phase in gravitational waves**Hajime Sotani,<sup>1,\*</sup> Nobutoshi Yasutake,<sup>1</sup> Toshiki Maruyama,<sup>2</sup> and Toshitaka Tatsumi<sup>3</sup><sup>1</sup>*Division of Theoretical Astronomy, National Astronomical Observatory of Japan, 2-21-1 Osawa, Mitaka, Tokyo 181-8588, Japan*<sup>2</sup>*Advanced Science Research Center, Japan Atomic Energy Agency, Tokai, Ibaraki 319-1195, Japan*<sup>3</sup>*Department of Physics, Kyoto University, Kyoto 606-8502, Japan*

(Received 28 October 2010; published 12 January 2011)

We calculate stellar oscillations, including the hadron-quark mixed phase, considering finite-size effects. We find that it is possible to distinguish whether the density discontinuity exists or not in the stars, even if one observes the gravitational waves of the fundamental mode. Additionally, the normalized eigenfrequencies of pressure modes depend strongly on the stellar mass and on the adopted equation of state. In particular, in spite of the fact that the radius of the neutron star with  $1.4M_{\odot}$ , which is the standard mass, is almost independent of the equation of state with quark matter, the frequencies of the pressure modes depend on the adopted equation of state. Thus, via observing the many kinds of gravitational waves, it will be possible to make a restriction on the equation of state.

DOI: [10.1103/PhysRevD.83.024014](https://doi.org/10.1103/PhysRevD.83.024014)

PACS numbers: 04.40.Dg, 97.60.Jd

**I. INTRODUCTION**

In order to detect gravitational waves, which are oscillations of spacetime itself, several ground-based detectors, such as LIGO, VIRGO, TAMA300, and GEO600, are in operation, and there are other projects that will build the next generation of detectors [1]. In addition to the ground-based detectors, some are also considering launching detectors in space, like LISA [2] and DECIGO [3]. Since the permeability of gravitational waves could be extremely strong, one can expect to see raw information of the wave sources via gravitational waves. On the other hand, the most promising sources of gravitational waves might be supernovae and mergers of binary compact objects; i.e., the gravitational waves are related to the compact stars, around which the gravitational field should be strong. So, the direct detection of gravitational waves could enable us not only to collect the astronomical data and to reveal the true properties of dense matter [4–11], but also to prove the gravitational theory in the strong-field regime [12,13].

In fact, an attempt to estimate the stellar parameters, such as mass, radius, and equation of state (EOS), via their oscillation properties is not a brand-new idea. In astronomy, the helioseismology has already been established, and one can see the interior information of our Sun through its oscillation properties. Since the late 1990s, it has been suggested that it is possible to reveal the compact star properties by observing the oscillation spectra; this is called gravitational wave asteroseismology [4,5]. Furthermore, the detailed analysis of the emitted gravitational waves might permit us to determine the radius of the accretion disk around supermassive black holes [14] or to see the magnetic effect during the stellar collapse [15].

With respect to the neutron stars, the density in the vicinity of the stellar center could become much more

than the standard nuclear density, which is around  $\rho_0 \approx 0.17 \text{ fm}^{-3}$ . Since such high density cannot be realized on the Earth, the detailed matter properties in neutron stars are still unknown. However, this means, conversely, that the neutron stars can be good candidates to find out the matter properties in the extreme high density region, where it is suggested that the exotic components of matter, such as hyperons, meson condensates, and quark matter, could appear [16]. The existence of these exotic components changes the EOS and neutron star structures dramatically [17–19]. Namely, as mentioned above, observing the stellar oscillations and/or the corresponding gravitational waves will tell us information about the matter properties of neutron stars. In particular, it might be impossible to probe the true properties of matter deep inside the star by any other experiments.

The hyperons are considered to appear at around  $2 - 3\rho_0$ , if the nuclear matter is in beta equilibrium [20,21]. On the other hand, there are still many uncertainties with respect to the hadron-quark phase transition, e.g., the EOS of quark matter or a deconfinement mechanism. The presence of quark matter inside the compact objects might play an important role in the astronomical phenomena, for example, the backbending effect from the phase transition [22,23], connection to gamma-ray bursts [24], gravitational wave bursts [25], gravitational radiation [26–29], energy release during the collapse from neutron stars to quark stars [30,31], neutrino luminosities [32–34], and cooling with quark matter [35–39]. Although Maxwell construction might be the simplest model with quark matter, the mixed phase could exist around the critical density that the quark matter appears, where baryon number and electric charge should be conserved. Generally, the properties of the mixed phase depend strongly on the electromagnetic interaction and the surface tension; these effects are called “the finite-size effects.” Because of the finite-size effects, the mixed phase is composed of a nonuniform

\*hajime.sotani@nao.ac.jp

pasta structure [18,19]. However, it is not clear how to distinguish the finite-size effects by observing the astronomical phenomena.

In this article, we study the gravitational waves emitted from compact stars with the hadron-quark mixed phase, considering the finite-size effects. Up to now, there exist a few studies from the gravitational wave asteroseismological point of view, which focus on probing the density discontinuity in the high density region using specific frequencies of gravitational waves (e.g., [7,8]). However, no one has investigated the effects of the mixed phase between the hadron and quark matter on the specific frequencies. So, in this article, preparing the neutron star models with the mixed phase or with density discontinuity between the hadron and quark matter phases, we will calculate the eigenfrequencies associated with the gravitational waves, where as a first step we adopt the Cowling approximation; i.e., the metric perturbation will be neglected. Then, by varying the stellar properties systematically, we will see the dependence of the existence of quark matter on the oscillation frequencies, considering finite-size effects.

This article is organized as follows. In the next section, we describe the equation system to construct the neutron star models and the EOS adopted in this article, and show some stellar models concretely. In Sec. III, we derive the perturbation equations with the Cowling approximation. With appropriate boundary conditions, the problem to solve becomes the eigenvalue problem. Then, the obtained oscillation spectra will be shown in Sec. IV. At last, we make a conclusion in Sec. V. In this article, we adopt units of  $c = G = 1$ , where  $c$  and  $G$  denote the speed of light and the gravitational constant, respectively, and the metric signature is  $(-, +, +, +)$ .

## II. NEUTRON STAR MODELS

The equilibrium configurations of nonrotating relativistic stars are spherically symmetric solutions of the well-known Tolman-Oppenheimer-Volkoff (TOV) equations. The metric can be expressed as

$$ds^2 = -e^{2\Phi} dt^2 + e^{2\Lambda} dr^2 + r^2 d\theta^2 + r^2 \sin^2\theta d\phi^2, \quad (2.1)$$

where  $\Phi$  and  $\Lambda$  are metric functions with respect to  $r$ . A mass function  $m(r)$  is defined as  $m(r) = r(1 - e^{-2\Lambda})/2$ , which satisfies

$$\frac{dm}{dr} = 4\pi r^2 \rho, \quad (2.2)$$

where  $\rho$  is the energy density, while the TOV equations used to determine the distributions of the pressure  $P(r)$  and metric function  $\Phi(r)$  are described as

$$\frac{dP}{dr} = -(\rho + P) \frac{d\Phi}{dr}, \quad (2.3)$$

$$\frac{d\Phi}{dr} = \frac{m + 4\pi r^3 P}{r(r - 2m)}. \quad (2.4)$$

To close the equation system, one needs an additional equation, i.e., the EOS.

In this article, we adopt an EOS with the hadron-quark mixed phase with hyperons, considering finite-size effects according to [18,19]. Our EOS for hadrons is in the framework of the nonrelativistic Brueckner-Hartree-Fock approach, including hyperons such as  $\Sigma^-$  and  $\Lambda$  [40]. It is not clear now whether the  $\Sigma^-$ - $N$  interaction is repulsive or not [41,42]; here we use a weak but attractive interaction. It would be interesting to see how our results are changed by using the other  $\Sigma^-$ - $N$  interactions, and we will discuss this in a future work. For comparison, we also adopt the EOS composed of only nucleons. We call them ‘‘hyperon EOS’’ and ‘‘nucleon EOS’’ in this article.

For the quark phase, we adopt the MIT bag model. It should be noticed that the adopted EOS in this article is not a simple MIT bag model but a more sophisticated model suggested in previous articles [43,44]. Assuming massless  $u$  and  $d$  quarks and  $s$  quarks with the current mass of  $m_s = 150$  MeV, we set the bag constant  $B$  to be  $100 \text{ MeV fm}^{-3}$ .

For the mixed phase, we assume nonuniform structures, so-called ‘‘pastas.’’ In practice, structures such as droplet, rod, slab, tube, and bubble are considered. We use the local density approximation for particles with the Wigner-Seitz cell. In order to construct such a pasta phase, we put a sharp boundary with a constant surface tension parameter between the hadron and quark phases. Then the Gibbs conditions are imposed, where one needs to solve two conditions: (1) the chemical equilibrium among particles in two phases consistent with the Coulomb potential, and (2) the pressure balance consistent with the surface tension. Although the knowledge of the value of the surface tension at the hadron-quark interface is very poor, some theoretical estimations have been done and they suggest that the value of the surface tension is around  $\sigma \approx 10\text{--}100 \text{ MeV/fm}^2$  [45,46]. Since one can see that the models with  $\sigma \geq 40 \text{ MeV/fm}^2$  are almost the same as that with  $\sigma = 40 \text{ MeV/fm}^2$ , in this article we consider only a range of  $10 \leq \sigma \leq 40 \text{ MeV/fm}^2$ . As an extreme case, we also consider the EOS with a Maxwell construction, which has a sharp discontinuity of the density between  $5.93 \times 10^{14}$  and  $8.82 \times 10^{14} \text{ g/cm}^3$ . Note that this discontinuity appears at strong surface tensions, considering finite-size effects, e.g.,  $\sigma > 70 \text{ MeV/fm}^2$  in our previous study [18]. Moreover, we take into account another extreme case of an EOS with the bulk Gibbs condition, which appears at the zero surface tension limit [18]. Finally, in order to determine which structure is most favored in the mixed phase, we compare the energy among the pasta structures. Note that we do not take into account the antiparticles and muons in this article, because their effects should not be so important.

Then the above EOSs should be connected to the hadronic EOS proposed by Negele and Vautherin [47] when the density becomes lower than around  $10^{14} \text{ g/cm}^3$ . In Table I, the components of each EOS adopted in this article

TABLE I. Components of each EOS adopted in this article.

EOS	Components
Nucleon	Nucleon
Hyperon	Nucleon, hyperon
Bulk Gibbs	Nucleon, hyperon, quark
With pasta phase	Nucleon, hyperon, quark
Maxwell	Nucleon, hyperon, quark

are summarized, while Fig. 1 shows the relationship between the energy density  $\rho$  and the pressure  $P$  in the higher density region for the EOSs adopted in this article. Solving the TOV equations with such EOSs, we can get the stellar properties as shown in Fig. 2. It should be noticed that the maximum masses of the stellar models constructed by EOSs including quark matter are almost independent of the values of  $\sigma$ , which are around  $1.4M_\odot$ . Here, we should discuss the maximum mass of neutron stars. Recently, two pulsar mass measurements appeared, which are well above  $1.4M_\odot$ , i.e.,  $M = 1.97M_\odot$  for PSR J1614-2230 [48] and  $M = 1.667M_\odot$  for PSR J1903 + 0327 [49]. Since it is impossible to explain these evidences with the EOS that includes quark matter, as adopted in this article, we should derive more realistic EOSs and examine the stellar oscillations in a future work.

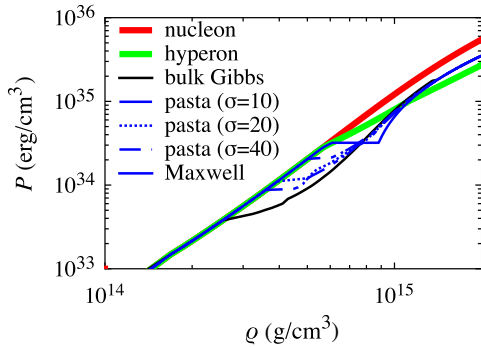


FIG. 1 (color online). Relationship between the total energy density including masses ( $\rho$ ) and the pressure ( $P$ ) for the EOSs adopted in this article.

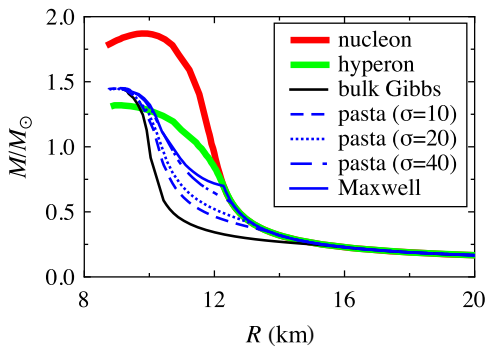


FIG. 2 (color online). Mass-radius relation for neutron stars with several EOSs.

### III. PERTURBATION EQUATIONS

In order to determine the specific oscillation frequencies in the neutron stars, in this section we present the perturbation equations for nonradial oscillations of spherically symmetric neutron stars. In particular, in this article we consider only stellar oscillations with the Cowling approximation, where the fluid would oscillate on a fixed background metric. Namely, the spacetime will be frozen such that the metric perturbation should be neglected ( $\delta g_{\mu\nu} = 0$ ). Thus, with the Cowling approximation, our study is limited to the modes related to the fluid perturbations, i.e.,  $f$ ,  $p$ , and  $g$  modes, while we cannot see the emission of gravitational waves associated with the so-called  $w$  modes which correspond to the spacetime oscillations. It should be emphasized that, even with this simple approximation, one can see qualitatively the features for oscillation frequencies of emitted gravitational waves.

The fluid Lagrangian displacement vector is given by

$$\xi^i = (e^{-\Lambda}W, -V\partial_\theta, -V\sin^{-2}\theta\partial_\phi)r^{-2}Y_{\ell m}, \quad (3.1)$$

where  $W$  and  $V$  are functions with respect to  $t$  and  $r$ , while  $Y_{\ell m}$  is the spherical harmonic function. Then the perturbations of the four-velocity,  $\delta u^\mu$ , can be written as

$$\delta u^\mu = (0, e^{-\Lambda}\partial_t W, -\partial_t V\partial_\theta, -\partial_t V\sin^{-2}\theta\partial_\phi)r^{-2}e^{-\Phi}Y_{\ell m}. \quad (3.2)$$

With these variables, the perturbation equations describing the fluid oscillations can be obtained by taking a variation of the energy-momentum conservation law, i.e.,  $\delta(\nabla_\nu T^{\mu\nu}) = 0$ . This equation reduces to  $\nabla_\nu \delta T^{\mu\nu} = 0$  with the Cowling approximation. The explicit forms with  $\mu = r, \theta$  are

$$\begin{aligned} \frac{\rho + P}{r^2}e^{\Lambda-2\Phi}\ddot{W} - \partial_r \left[ \frac{\gamma P}{r^2} \{e^{-\Lambda}W' + \ell(\ell+1)V\} + e^{-\Lambda}P' \frac{W}{r^2} \right] \\ + \frac{P'}{r^2} \left( 1 + \frac{dP}{d\rho} \right) [e^{-\Lambda}W' + \ell(\ell+1)V] \\ - \frac{\rho' + P'}{r^2} \Phi' e^{-\Lambda}W = 0, \end{aligned} \quad (3.3)$$

$$\begin{aligned} (\rho + P)e^{-2\Phi}\ddot{V} + \frac{\gamma P}{r^2} [e^{-\Lambda}W' + \ell(\ell+1)V] \\ + \frac{P'}{r^2} e^{-\Lambda}W = 0, \end{aligned} \quad (3.4)$$

where primes and dots on the variables denote the partial derivatives with respect to  $r$  and  $t$ , respectively.  $\gamma$  is the adiabatic constant defined as

$$\gamma \equiv \left( \frac{\partial \ln P}{\partial \ln n} \right)_s = \frac{n\Delta P}{P\Delta n}, \quad (3.5)$$

where  $n$  is the baryon number density and  $\Delta$  denotes the Lagrangian variation. The Lagrangian variation of the baryon number density,  $\Delta n$ , is determined by the relation

$\Delta n/n = -\nabla_k^{(3)} \xi^k - \delta g/g$ , where  $\nabla_k^{(3)}$  and  $g$  are the covariant derivatives in three dimensions with the metric  $g_{\mu\nu}$  and the determinant of  $g_{\mu\nu}$ , respectively. Since in this article we adopt the Cowling approximation, the second term is neglected. Then the Lagrangian variation of  $n$  can be described as

$$\frac{\Delta n}{n} = -e^{-\Lambda} \frac{W'}{r^2} - \frac{\ell(\ell+1)}{r^2} V. \quad (3.6)$$

Assuming a harmonic dependence on time, the perturbative variables will be written as  $W(t, r) = W(r)e^{i\omega t}$  and  $V(t, r) = V(r)e^{i\omega t}$ . Additionally, calculating the combination of the form  $d[\text{Eq.}(3.4)]/dr - [\text{Eq.}(3.3)]$  and substituting Eq. (3.4) again, one can get the simple equation

$$V' = 2\Phi'V - e^\Lambda \frac{W}{r^2}. \quad (3.7)$$

Thus, from Eqs. (3.4) and (3.7), one can obtain the following simple equation system for the fluid perturbations:

$$W' = \frac{d\rho}{dP} [\omega^2 r^2 e^{\Lambda-2\Phi} V + \Phi'W] - \ell(\ell+1)e^\Lambda V, \quad (3.8)$$

$$V' = 2\Phi'V - e^\Lambda \frac{W}{r^2}. \quad (3.9)$$

In order to solve this equation system, we have to impose appropriate boundary conditions at the stellar center ( $r=0$ ) and at the stellar surface ( $r=R$ ). With these boundary conditions, the problem to solve becomes an eigenvalue problem for the parameter  $\omega$ . From the above equation system, one can find the behavior of  $W$  and  $V$  in the vicinity of the stellar center as  $W(r) = Cr^{\ell+1} + \mathcal{O}(r^{\ell+3})$  and  $V(r) = -Cr^\ell/\ell + \mathcal{O}(r^{\ell+2})$ , where  $C$  is an arbitrary constant. On the other hand, the boundary condition at the stellar surface is the vanishing of the Lagrangian perturbation of pressure, i.e.,  $\Delta P = 0$ . Since  $\Delta P$  could be expressed as  $\Delta P = \gamma P \Delta n/n$  from Eq. (3.5), with the help of Eqs. (3.6) and (3.8), the condition of  $\Delta P = 0$  becomes

$$\omega^2 r^2 e^{\Lambda-2\Phi} V + \Phi'W = 0. \quad (3.10)$$

Furthermore, if one considers the stellar models with density discontinuity, one has to prepare the additional junction conditions at the surface of discontinuity, which are the continuous conditions for  $W$  and  $\Delta P$  [7]. These junction conditions can be rewritten with the variables  $W$  and  $V$  as

$$W_+ = W_-, \quad (3.11)$$

$$V_+ = \frac{e^{2\Phi}}{\omega^2 R_g^2} \left\{ \frac{\rho_- + P}{\rho_+ + P} [\omega^2 R_g^2 e^{-2\Phi} V_- + e^{-\Lambda} \Phi' W_-] - e^{-\Lambda} \Phi' W_+ \right\}, \quad (3.12)$$

where  $R_g$  denotes the position of the density discontinuity, and  $W_-$ ,  $V_-$ , and  $\rho_-$  are the values of  $W$ ,  $V$ , and  $\rho$  at  $r = R_g - 0$ , while  $W_+$ ,  $V_+$ , and  $\rho_+$  are the values of  $W$ ,  $V$ , and  $\rho$  at  $r = R_g + 0$ , respectively.

#### IV. OSCILLATION SPECTRA

In this section we examine the stellar oscillations on the stellar models shown in Sec. II. In particular, we focus on the stellar models whose mass is in the range of  $0.5M_\odot \leq M \leq M_{\max}$  and at  $0.1M_\odot$  intervals, where  $M_{\max}$  is the maximum mass for each EOS. Namely, the masses of the stellar models we adopt in this article are  $0.5 \leq M/M_\odot \leq 1.3$  for the hyperon EOS,  $0.5 \leq M/M_\odot \leq 1.8$  for the nucleon EOS, and  $0.5 \leq M/M_\odot \leq 1.4$  for the other EOSs. As mentioned above, the stellar models with Maxwell EOSs have the density discontinuity, if the central density is larger than  $8.816 \times 10^{14} \text{ g/cm}^3$ . That is, for Maxwell EOSs, the stellar models with  $0.7 \leq M/M_\odot \leq 1.4$  have the density discontinuity, while those with  $M/M_\odot = 0.5$  and  $0.6$  do not have the density discontinuity, and such stellar models are the same as those with hyperon EOSs (see Fig. 2).

When neutron stars oscillate, many kinds of gravitational waves are radiated. If the stars are spherically symmetric and without density discontinuity inside the star, which might be the simplest model, the fundamental ( $f$ ), pressure ( $p$ ), and spacetime ( $w$ ) modes are excited, where  $f$  and  $p$  modes are gravitational waves related to the fluid oscillations while  $w$  modes correspond to the oscillations of spacetime itself. If the stars are spherically symmetric and with density discontinuity, the additional oscillation modes, i.e., the  $g$  modes, are excited as well as  $f$ ,  $p$ , and  $w$  modes. The  $g$  modes are also gravitational waves associated with the fluid oscillations. In this article, we will see qualitatively the gravitational waves related to the fluid oscillations because the Cowling approximation is adopted in our analysis. Thus, as shown in Fig. 3, the stellar models with the adopted EOSs, except for the Maxwell EOS, have  $f$  and  $p$  modes, while those with the Maxwell EOS, whose masses are more than  $0.7M_\odot$ , have  $f$ ,  $p$ , and  $g$  modes.

Before discussing the  $f$  and  $p$  modes, we pay attention to the  $g$  mode for the stellar models with Maxwell EOSs. As noted before, the  $g$  mode is excited due to the existence of density discontinuity. Therefore, one could know about the existence of density discontinuity inside the neutron stars, if the  $g$  mode gravitational waves are observed. Actually, since the typical frequency of the  $g$  mode is in the range from a few hundred Hz up to kHz, such gravitational waves could be observed by using the ground-based gravitational wave detectors. From Fig. 3, one can observe that the frequency of the  $g$  mode is almost independent of the stellar mass, which is around 1.73 Hz. However, we find that the  $g$  mode frequency can be expressed well as a function of stellar compactness  $M/R$  (see Fig. 4), such as



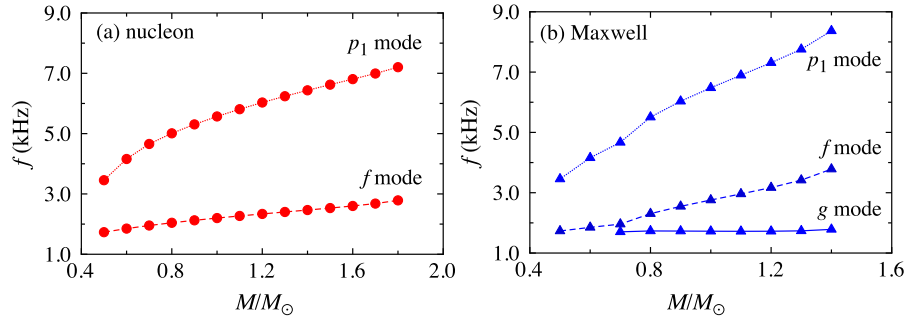


FIG. 3 (color online). The first few eigenfrequencies for the stellar models with (a) nucleon and (b) Maxwell EOSs are plotted as a function of the stellar mass  $M/M_\odot$ , where the frequency  $f$  is defined as  $f \equiv \omega/2\pi$ . As mentioned in the text, for the case of the stellar models with the other EOSs, the excited eigenfrequencies are the same as in the case of the stellar model with nucleon EOSs; i.e., they have  $f$  and  $p_i$  modes, where  $i = 1, 2, 3, \dots$ . On the other hand, the stellar model with the Maxwell EOS, which has a first order phase transition in the density, has an additional eigenfrequency, which is the  $g$  mode.

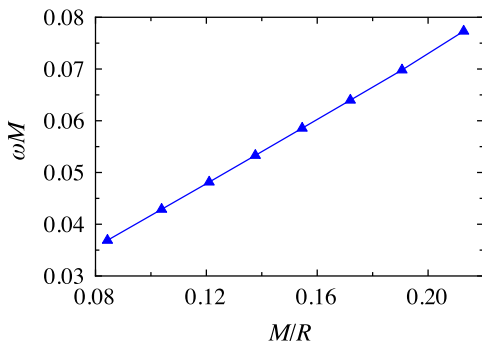


FIG. 4 (color online). The normalized eigenvalue  $\omega$  of the  $g$  mode for the stellar models with Maxwell EOSs are plotted as a function of the stellar compactness  $M/R$ .

$$\omega M = 0.3130 \left( \frac{M}{R} \right) + 0.0103. \quad (4.1)$$

Practically, from this empirical formula, we can expect the  $g$  mode frequency with less than 0.6% accuracy. So, via observing the  $g$  mode gravitational waves, one could know the stellar properties. Or, with the observation of the redshift parameter, which is connected to the stellar

compactness directly, one could make a restriction on the stellar mass.

On the other hand, it is well known that the frequency of the  $f$  mode can be connected to the stellar average density  $(M/R^3)^{1/2}$ , which could be physically explained by considering the relation between the sound speed and the propagation time of the fluid perturbation inside the star. In fact, Andersson and Kokkotas derived the empirical formula for the  $f$  mode frequency by performing calculations in the stellar models with several realistic EOSs [5]. Although they did not adopt the EOS including the quark matter, they found that the  $f$  mode frequencies obtained in their article are subject to their empirical formula almost independently of the EOS. However, in Fig. 5, we show the  $f$  mode frequencies for the stellar models with EOSs adopted in this article. At a glance, one can observe that the behavior of the  $f$  mode frequencies for the stellar models with the Maxwell EOS is quite different from the others. The  $f$  mode frequencies for the Maxwell EOS could become 36% larger than those for nucleon EOS and 27% larger than those for the other EOSs. This means that one could possibly know about the existence of the density discontinuity even by observing the  $f$  mode

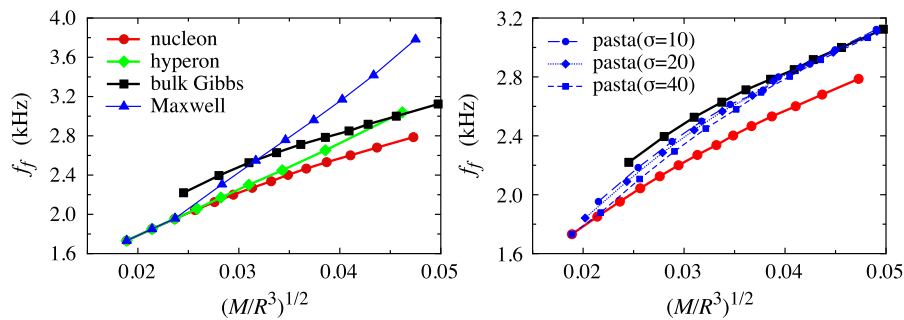


FIG. 5 (color online). With several EOSs, the frequencies of the  $f$  modes are plotted as a function of the stellar average density  $(M/R^3)^{1/2}$ , where  $f_f$  is defined as  $f_f \equiv \omega_f/2\pi$ . The left panel corresponds to the results with nucleon, hyperon, bulk Gibbs, and Maxwell EOSs, while the right panel focuses on the pasta EOSs.

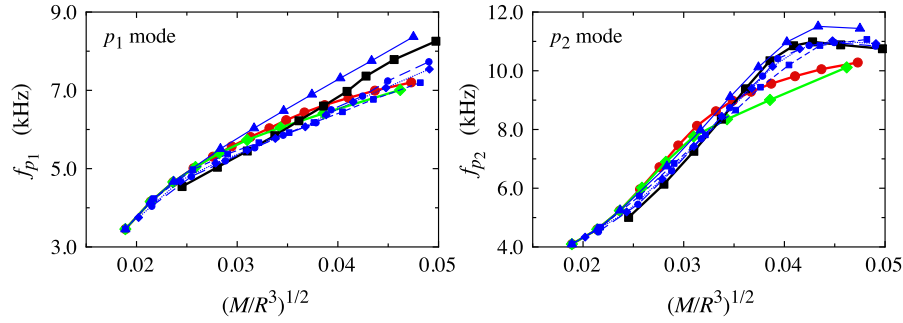


FIG. 6 (color online). With several EOSs, the frequencies of  $p_1$  (left panel) and  $p_2$  (right panel) modes are plotted as a function of the stellar average density  $(M/R^3)^{1/2}$ , where the marks in the figures correspond to those in Fig. 5.

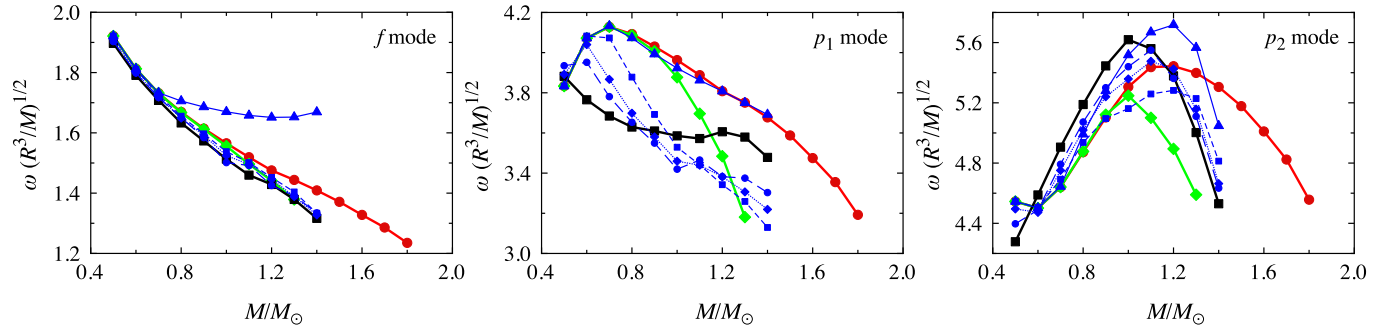


FIG. 7 (color online). The normalized eigenvalues of  $f$  (left panel),  $p_1$  (middle panel), and  $p_2$  (right panel) modes are plotted as a function of the stellar mass  $M/M_\odot$ , where the marks in the figures correspond to those in Fig. 5.

gravitational waves as well as the  $g$  mode ones. Additionally, Fig. 5 shows that the  $f$  modes for the stellar models with pasta EOSs are similar to those for the stellar models with the other EOSs without density discontinuity.

Regarding the  $p$  modes, we plot the frequencies of the  $p_1$  and  $p_2$  modes as functions of the average density in Fig. 6. From this figure, one can see that the  $p_i$  mode frequencies are almost independent of the EOS even if it includes the density discontinuity. However, one can see the dependence of the  $p$  mode frequency on the EOS if we prepare the figure with regards to the normalized eigenvalues with average density,  $\omega(R^3/M)^{1/2}$ , as a function of the stellar mass (see Fig. 7). The most interesting point in this figure is that the normalized eigenvalues for the stellar models with  $1.4M_\odot$  depend strongly on the adopted EOS, in spite of the fact that the stellar shapes are almost independent of the adopted EOSs including quark matter, i.e.,  $R = 9.42\text{--}9.67$  km. Moreover, in this figure, the dependence of the normalized eigenvalues of the  $p_1$  mode on the EOS is different from that of the  $p_2$  modes. Thus, with the help of the observations of stellar mass, it could be possible to distinguish the EOSs by observing the several kinds of oscillation modes. At last, it should also be noticed that the normalized eigenvalues of the  $f$  modes for the stellar model with the Maxwell EOS are obviously different from the other stellar models as well as Fig. 5.

## V. CONCLUSION

We study how to distinguish the finite effects on the hadron-quark mixed phase by observing gravitational waves, for which we derive the perturbation equations of neutron stars and obtain their eigenfrequencies.

We find that one could know about the existence of density discontinuity inside the star via observing the gravitational waves of not only the  $g$  mode but also the  $f$  mode. Note that this discontinuity comes from the instability of the mixed phase due to the strong surface tension. Additionally, it is possible to see the stellar properties by observing the  $g$  mode frequency, since such a frequency can be expressed well as a function of the stellar compactness. If the EOSs do not include the density discontinuity, it might be difficult to distinguish the EOSs by only observing the  $f$  mode frequencies. However, the normalized eigenfrequencies of the  $p$  modes depend strongly on the EOSs even if the EOSs do not include the density discontinuity, although the raw frequencies of the  $p$  mode are almost independent. Thus, with the help of the observation of stellar properties, it could be possible to make a restriction on the stellar EOSs.

In this article, for simplicity, we assume the Cowling approximation, which restricts our examination to only stellar oscillations. This means that we should do a more detailed study including the metric perturbations. Via this

type of oscillation, we could obtain additional information, such as the damping rate of gravitational waves, and combining this with results shown in this article would provide more accurate constraints on the stellar properties and/or the stellar EOSs. Furthermore, the stellar magnetic field might play an important role. For example, quasiperiodic oscillations have been observed in the giant flare, and these phenomena are believed to be oscillations of strong magnetized neutron stars [50]. Considering the effects of stellar magnetic fields, it might be possible to obtain further information.

Additionally, although we focus only on neutron star matter ( $T = 0$  MeV and  $Y_{\nu_e} = 0$ ) in this article, in order to study the protoneutron stars, we should take into account other effects, e.g., the thermal effects on the stellar

oscillations [51] and the effects of temperature and/or neutrino trapping on the pasta structures [19,52,53].

## ACKNOWLEDGMENTS

We are grateful to Y. Sekiguchi, S. Chiba, H.-J. Schulze, G. F. Burgio, and M. Baldo for their warm hospitality and fruitful discussions, and also to the referee for valuable comments. This work was partially supported by the Grant-in-Aid for the Global COE Program “The Next Generation of Physics, Spun from Universality and Emergence,” from the Ministry of Education, Culture, Sports, Science and Technology (MEXT) of Japan, and the Grant-in-Aid for Scientific Research (C) (20540267, 21105512, 19540313).

- 
- [1] B. C. Barich, in *Proceedings of the 17th International Conference on General Relativity and Gravitation*, edited by P. Florides, B. Nolan, and A. Ottewill (World Scientific, New Jersey, 2005), p. 24.
  - [2] <http://lisa.jpl.nasa.gov/>.
  - [3] S. Kawamura *et al.*, *Classical Quantum Gravity* **23**, S125 (2006).
  - [4] N. Andersson and K. D. Kokkotas, *Phys. Rev. Lett.* **77**, 4134 (1996).
  - [5] N. Andersson and K. D. Kokkotas, *Mon. Not. R. Astron. Soc.* **299**, 1059 (1998).
  - [6] K. D. Kokkotas, T. A. Apostolatos, and N. Andersson, *Mon. Not. R. Astron. Soc.* **320**, 307 (2001).
  - [7] H. Sotani, K. Tominaga, and K. I. Maeda, *Phys. Rev. D* **65**, 024010 (2001).
  - [8] G. Miniutti *et al.*, *Mon. Not. R. Astron. Soc.* **338**, 389 (2003).
  - [9] H. Sotani and T. Harada, *Phys. Rev. D* **68**, 024019 (2003); H. Sotani, K. Kohri, and T. Harada, *ibid.* **69**, 084008 (2004).
  - [10] M. Vavoulidis, K. D. Kokkotas, and A. Stavridis, *Mon. Not. R. Astron. Soc.* **384**, 1711 (2008).
  - [11] E. Gaertig and K. D. Kokkotas, *Phys. Rev. D* **80**, 064026 (2009).
  - [12] H. Sotani and K. D. Kokkotas, *Phys. Rev. D* **70**, 084026 (2004); **71**, 124038 (2005).
  - [13] H. Sotani, *Phys. Rev. D* **79**, 064033 (2009); **80**, 064035 (2009).
  - [14] H. Sotani and M. Saijo, *Phys. Rev. D* **74**, 024001 (2006).
  - [15] H. Sotani, S. Yoshida, and K. D. Kokkotas, *Phys. Rev. D* **75**, 084015 (2007); H. Sotani, *ibid.* **79**, 084037 (2009).
  - [16] H. Heiselberg and M. Hjorth-Jensen, *Phys. Rep.* **328**, 237 (2000).
  - [17] G. F. Burgio, M. Baldo, P. K. Sahu, and H. -J. Schulze, *Phys. Rev. C* **66**, 025802 (2002).
  - [18] T. Maruyama, S. Chiba, H. J. Schulze, and T. Tatsumi, *Phys. Rev. D* **76**, 123015 (2007).
  - [19] N. Yasutake, T. Maruyama, and T. Tatsumi, *Phys. Rev. D* **80**, 123009 (2009).
  - [20] C. Ishizuka *et al.*, *J. Phys. G* **35**, 085201 (2008).
  - [21] H.-J. Schulze, A. Polls, A. Ramos, and I. Vidaña, *Phys. Rev. C* **73**, 058801 (2006).
  - [22] N. K. Glendenning, S. Pei, and F. Weber, *Phys. Rev. Lett.* **79**, 1603 (1997).
  - [23] J. L. Zdunik, M. Bejger, P. Haensel, and E. Gourgoulhon, *Astron. Astrophys.* **450**, 747 (2006).
  - [24] A. Drago and G. Pagliara, *Astrophys. J.* **665**, 1227 (2007).
  - [25] A. Drago, G. Pagliara, and Z. Berezhiani, *Astron. Astrophys.* **445**, 1053 (2006).
  - [26] R. Oechslin, K. Uryu, G. Poghosyan, and F. K. Thielemann, *Mon. Not. R. Astron. Soc.* **349**, 1469 (2004).
  - [27] F. Limousin, D. Gondek-Rosinska, and E. Gourgoulhon, *Phys. Rev. D* **71**, 064012 (2005).
  - [28] L.-M. Lin, K. S. Cheng, M. C. Chu, and W.-M. Suen, *Astrophys. J.* **639**, 382 (2006).
  - [29] N. Yasutake, K. Kotake, M. A. Hashimoto, and S. Yamada, *Phys. Rev. D* **75**, 084012 (2007).
  - [30] N. Yasutake, M. Hashimoto, and Y. Eriguchi, *Prog. Theor. Phys.* **113**, 953 (2005).
  - [31] N. Yasutake, K. Kiuchi, and K. Kotake, *Mon. Not. R. Astron. Soc.* **401**, 2101 (2010).
  - [32] T. Hatsuda, *Mod. Phys. Lett. A* **2**, 805 (1987).
  - [33] K. Nakazato, K. Sumiyoshi, and S. Yamada, *Phys. Rev. D* **77**, 103006 (2008).
  - [34] I. Sagert *et al.*, *Phys. Rev. Lett.* **102**, 081101 (2009).
  - [35] D. Page, M. Prakash, J. M. Lattimer, and A. W. Steiner, *Phys. Rev. Lett.* **85**, 2048 (2000).
  - [36] H. Grigorian, D. Blaschke, and D. Voskresensky, *Phys. Rev. C* **71**, 045801 (2005).
  - [37] M. Alford, P. Jotwani, C. Kouvaris, J. Kundu, and K. Rajagopal, *Phys. Rev. D* **71**, 114011 (2005).
  - [38] M. Kang and X. Zheng, *Mon. Not. R. Astron. Soc.* **375**, 1503 (2007).
  - [39] M. Stejner, F. Weber, and J. Madsen, *Astrophys. J.* **694**, 1019 (2009).

- [40] M. Baldo, G. F. Burgio, and H.-J. Schulze, *Phys. Rev. C* **58**, 3688 (1998).
- [41] H. Noumi *et al.*, *Phys. Rev. Lett.* **89**, 072301 (2002).
- [42] P. K. Saha *et al.*, *Phys. Rev. C* **70**, 044613 (2004).
- [43] N. Yasutake and K. Kashiwa, *Phys. Rev. D* **79**, 043012 (2009).
- [44] H. Chen *et al.*, *Phys. Rev. D* **78**, 116015 (2008).
- [45] E. Farhi and R. L. Jaffe, *Phys. Rev. D* **30**, 2379 (1984).
- [46] K. Kajantie, L. Kärkäinen, and K. Rummukainen, *Nucl. Phys.* **B357**, 693 (1991).
- [47] J. W. Negele and D. Vautherin, *Nucl. Phys.* **A207**, 298 (1973).
- [48] P. Demorest, T. Pennucci, S. Ransom, M. Roberts, and J. Hessels, *Nature (London)* **467**, 1081 (2010).
- [49] P. C. C. Freire *et al.*, [arXiv:1011.5809](https://arxiv.org/abs/1011.5809) [*Mon. Not. R. Astron. Soc.* (to be published)].
- [50] H. Sotani, K. D. Kokkotas, and N. Stergioulas, *Mon. Not. R. Astron. Soc.* **375**, 261 (2007); **385**, L5 (2008); H. Sotani, A. Colaiuda, and K. D. Kokkotas, *ibid.* **385**, 2161 (2008); H. Sotani and K. D. Kokkotas, *ibid.* **395**, 1163 (2009).
- [51] P. N. McDermott, H. M. Van Horn, and C. J. Hansen, *Astrophys. J.* **325**, 725 (1988).
- [52] G. Pagliara, M. Hempel, and J. Schaffner-Bielich, *Phys. Rev. Lett.* **103**, 171102 (2009).
- [53] M. Hempel, G. Pagliara, and J. Schaffner-Bielich, *Phys. Rev. D* **80**, 125014 (2009).